Coexistent quantum and classical aspects of magnetization plateaux in alternating-spin chains

2000 J. Phys.: Condens. Matter 12 9787

(http://iopscience.iop.org/0953-8984/12/47/306)

J. Phys.: Condens. Matter **12** (2000) 9787–9797. Printed in the UK PII: S0953-8984(00)13917-7

Coexistent quantum and classical aspects of magnetization plateaux in alternating-spin chains

Tôru Sakai† and Shoji Yamamoto‡

† Faculty of Science, Himeji Institute of Technology, Kamigori, Hyogo 678-1297, Japan
‡ Department of Physics, Okayama University, Tsushima, Okayama 700-8530, Japan

Received 16 May 2000, in final form 12 September 2000

Abstract. The processes of magnetization of ferrimagnetic Heisenberg chains of alternating spins are studied theoretically. Size-scaling analysis with the exact diagonalization of finite systems for $(S, s) = (3/2, 1)$ and $(2, 1)$ indicates a multi-plateau structure in the ground-state magnetization curve for S and $s > 1/2$. The first plateau in the spontaneous magnetization can be explained classically: as originating from the Ising gap. In contrast, the second and higher ones must be originating from the quantization of the magnetization. It is also found that all of the $2s$ plateaux, both classical and quantum ones, appear even in the isotropic case with no bond alternation.

1. Introduction

Alternating spin chains with antiferromagnetic interactions are currently attracting a lot of attention. The optical mode of the low-lying excitation indicates that they behave like gapped antiferromagnets, while they also exhibit a ferromagnetic aspect characterized by a spontaneous magnetization. The coexistence of the two aspects gives rise to various interesting crossover phenomena at low temperatures (Yamamoto 2000). However, few *quantum* aspects have ever been reported on for these systems. Hence we consider an interesting phenomenon caused by a quantum mechanism, called *quantization of magnetization*, in the framework of quantum ferrimagnetic chains. This would be observed as a plateau in the ground-state magnetization curve. Recently, many theoretical (Oshikawa *et al* 1997, Totsuka 1998, Tonegawa *et al* 1996, Cabra *et al* 1997, Cabra and Grynberg 1999, Sakai and Takahashi 1998) and experimental (Narumi *et al* 1998, Shiramura *et al* 1998) studies have suggested the realization of magnetization plateaux in various systems.

Previous works (Yamamoto and Sakai 1999, Sakai and Yamamoto 1999) by the present authors indicated an important role for quantum fluctuation in stabilizing the plateau against planar anisotropy in the ferrimagnetic chain. This results in the plateau existing even in the XY model of the mixed spins 1 and 1/2. On the other hand, the classical mixed-spin systems have the same plateau in the isotropic case. This implies that the plateau was originally produced by a classical mechanism, although it is stabilized by a quantum effect. Thus it is difficult to say whether the plateau symbolizes the quantum nature of the ferrimagnetic chains. In the present paper, other plateaux, essentially based on a *quantum* mechanism, are revealed to coexist with the above-mentioned *classical* plateau, when both spins are larger than 1/2.

0953-8984/00/479787+11$30.00

2. Quantum and classical plateaux

A recent exact treatment (Oshikawa *et al* 1997) for general quantum spin chains suggested that a magnetization plateau can appear as a result of the quantization of the magnetization under the condition

$$S_{\text{unit}} - m = \text{integer} \tag{1}$$

where S_{unit} and m are the total spin and magnetization per unit cell. Note that relation (1) is only a necessary condition. Thus it does not guarantee the existence of the plateau nor specify any mechanism of formation. Condition (1) is still valid for mixed-spin chains of spins S and s ($S > s$), described by the Hamiltonian

$$\mathcal{H} = \sum_{j=1}^{N}\left[(1+\delta)(\boldsymbol{S}_j \cdot \boldsymbol{s}_j)_\alpha + (1-\delta)(\boldsymbol{s}_j \cdot \boldsymbol{S}_{j+1})_\alpha - H(S_j^z + s_j^z)\right] \tag{2}$$

with $(\boldsymbol{S} \cdot \boldsymbol{s})_\alpha = S^x s^x + S^y s^y + \alpha S^z s^z$. In the isotropic case ($\alpha = 1$) with no bond alternation ($\delta = 0$), the system has a spontaneous magnetization $m_s \equiv S - s$. Because of the antiferromagnetic gap, the ground state with magnetization m_s is so stable against the excitation increasing m that a magnetization plateau appears at $m = m_s$ (Kuramoto 1998). Previous works (Yamamoto and Sakai 1999, Sakai and Yamamoto 1999) on the most quantized system, $(S, s) = (1, 1/2)$, suggested that the quantum fluctuation stabilizes the plateau against XY-like anisotropy ($\alpha < 1$) and that the plateau phase extends to the Kosterlitz–Thouless phase boundary in the ferromagnetic region ($\alpha < 0$). However, this plateau phase also includes the Ising limit ($\alpha \to \infty$) without any other boundaries. Thus it is difficult to establish that certain effects on the plateau formation are quantum effects, because they cannot be clearly distinguished from those of the Ising gap resulting from a classical mechanism. In fact, the classical spin (vector) model with the same magnitudes $(S, s) = (1, 1/2)$, described by the same Heisenberg Hamiltonian (2), also has a plateau at $m = m_s$ for $\alpha = 0$. Thus the plateau at m_s could be called a *classical plateau*. On the other hand, the condition of quantization (1) suggests that some other plateaux can appear at higher magnetizations $m = S - s + 1, S - s + 2, \ldots, S + s - 1$ for $S > s > 1/2$. These higher plateaux can never be explained by any classical mechanisms, because they cannot appear in the Ising model or classical Heisenberg model. Thus they should be called *quantum plateaux*, if they do in fact appear. In the following sections, we perform some theoretical analyses for the systems with $(S, s) = (3/2, 1)$ and $(2, 1)$ to establish the coexistence of the quantum and classical plateaux in the case of $S > s > 1/2$.

3. Low-lying excitations

The optical mode of the low-lying excitations characterizes the features of the initial plateau at m_s. In figure 1 we show the excitation spectra of the systems (a) $(3/2, 1)$ and (b) $(2, 1)$ for $\alpha = 1$ and $\delta = 0$, derived by three methods: quantum Monte Carlo (QMC) simulation; modified spin-wave theory; and perturbation from the decoupled dimer. The first one gives the most precise results and the last one is based on the dimer state described as $\prod_j (A_j^\dagger)^{S-s}(A_j^\dagger b_j^\dagger - B_j^\dagger a_j^\dagger)^{2s}|0\rangle$, making use of the Schwinger boson representation:

$$\begin{aligned} S_j^+ &= A_j^\dagger B_j \qquad & S_j^z &= \frac{1}{2}(A_j^\dagger A_j - B_j^\dagger B_j) \\ s_j^+ &= a_j^\dagger b_j \qquad & s_j^z &= \frac{1}{2}(a_j^\dagger a_j - b_j^\dagger b_j). \end{aligned} \tag{3}$$

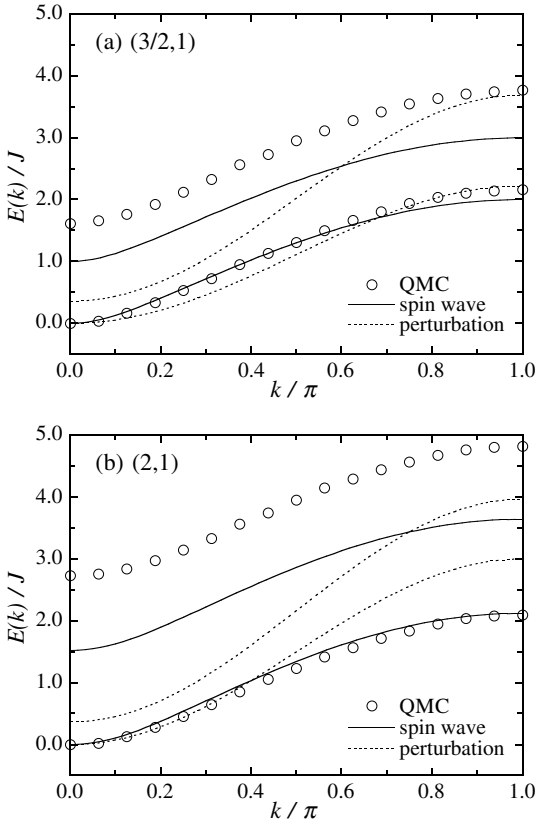

Figure 1. Low-lying excitation spectra calculated by quantum Monte Carlo (QMC) simulation, from spin-wave theory and by perturbation from the decoupled dimer for (a) (3/2, 1) and (b) (2, 1).

The excitation spectrum of each system has two branches characterizing the ferromagnetic (lower) and antiferromagnetic (upper) features, as well as the system $(1, 1/2)$ itself. The calculated curves suggest that the spin wave is more suitable than the decoupled dimer for describing the behaviour of the optical branch around its bottom ($k = 0$). This implies that the classical picture (spin-wave excitation from the Néel order) is more suitable than the quantum one (dimer-breaking excitation) for explaining the origin of the initial plateau, as expected from the above argument.

4. The variational approach

According to the condition of quantization (1), the mixed-spin chains $(3/2, 1)$ and $(2, 1)$ may have two plateaux at $m = m_s$ and $m_s + 1$. In order to characterize these plateaux, we introduce a variational wave function for the ground state of the model (2) as follows:

$$|\mathrm{g}\rangle = c_{\mathrm{N}} \prod_{j=1}^{N} (A_j^\dagger)^{2S} (b_j^\dagger)^{2s} |0\rangle + \sum_{l=0}^{2s} c_{\mathrm{VB}}^{(l)} \prod_{j=1}^{N} (A_j^\dagger)^{2S-l} (a_j^\dagger)^{2s-l} (A_j^\dagger b_j^\dagger - B_j^\dagger a_j^\dagger)^l |0\rangle \tag{4}$$

where c_{N} and $c_{\mathrm{VB}}^{(l)}$ are the mixing coefficients. Using the variational wave function, the ground-state phase diagram in the H–δ plane is obtained, as shown in figures 2(a) and 2(b) for $(3/2, 1)$

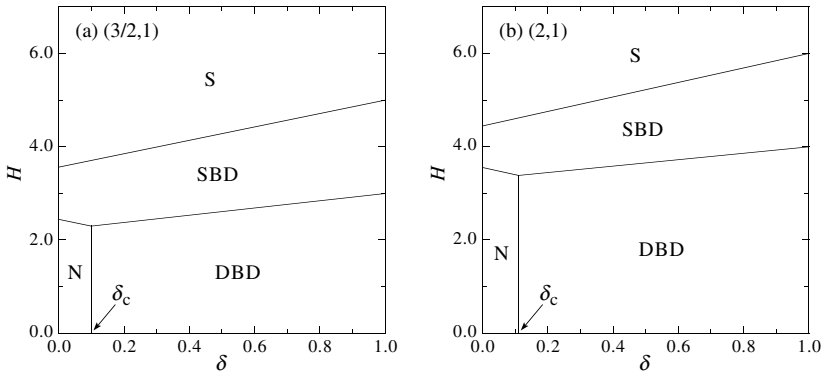

Figure 2. The variational ground-state phase diagrams in the δ–H plane with $\alpha = 1$ for (a) $(3/2, 1)$ and (b) $(2, 1)$. The phases are denoted as follows: N: Néel; DBD: double-bond dimer; SBD: single-bond dimer; and S: saturation.

and $(2, 1)$, respectively, where we restrict consideration to the Heisenberg point ($\alpha = 1$). In the first step of the magnetization process for each system, there exists a crossover point δ_c between the Néel (N) and double-bond dimer (DBD) states. In contrast, the second step toward saturation (S) is always a single-bond dimer (SBD) state. These two steps before saturation is reached are expected to characterize the two plateaux. Thus the first plateau should be based on the classical Néel order, while the second one should be based on the quantum valence-bond-solid state, as long as we consider the case of small δ.

5. Phase diagrams

In order to confirm the coexistence of the two plateaux even for $\alpha = 1$ and $\delta = 0$, we perform a size-scaling analysis with the exact diagonalization of finite systems up to $N = 12$ to obtain the phase diagrams in the δ–α plane. $E(N, M)$ denotes the lowest energy in the subspace with a fixed magnetization M for the Hamiltonian (2) without the Zeeman term. The upper and lower bounds of the external field which induces the ground-state magnetization M are expressed as $H_{\pm}(N, M) = \pm E(N, M \pm 1) \mp E(N, M)$. The length of the plateau with the unit-cell magnetization $m \equiv M/N$ is obtained as $\Delta_N(m) = H_+(N, M) - H_-(N, M)$. The quantity $\Delta_N(m)$ also corresponds to the sum of the two excitation gaps for increasing and reducing the magnetization (Sakai and Takahashi 1998). Thus the scaled quantity $N\Delta_N(m)$ is a good probe of the plateau. The lack of size dependence has the result that the system is gapless. The scaled quantity for the system $(3/2, 1)$ is shown as a function of α for $\delta = 0$ at (a) $m = 1/2$ and (b) $m = 3/2$ in figure 3. Figure 3(a) clearly shows that the opening plateau at around $\alpha = 1$ vanishes at some critical value α_c for $m = 1/2$ and that there is a gapless phase in the region of $\alpha < \alpha_c$. The scaled gap in figure 3(b) also indicates the existence of the second plateau around $\alpha = 1$, although the size dependence is much smaller than that of the first plateau. This implies that the second plateau is much smaller than the first one.

To investigate the critical properties around α_c, we use the size-scaling formula based on conformal field theory (Cardy 1984, Blöte *et al* 1986, Affleck 1986):

$$\frac{1}{N}E(N, M) \sim \epsilon(m) - \frac{\pi v_s c}{6N^2} \tag{5}$$

and

$$\Delta_N(m) \sim \frac{\pi v_s \eta}{N} \tag{6}$$

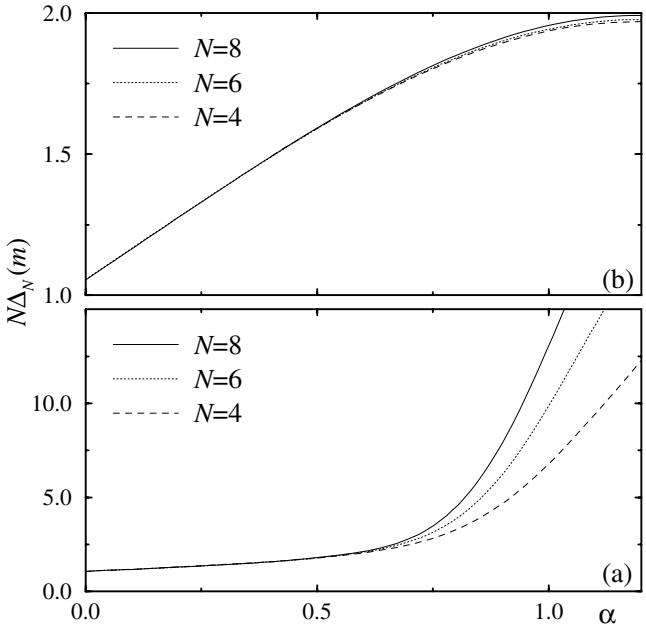

Figure 3. The scaled quantity $N\Delta_N(m)$ versus α at $m = 1/2$ (a) and $m = 3/2$ (b) in the case of $(S, s) = (3/2, 1)$.

with the following notation: $\epsilon(m)$ is the ground-state energy of the bulk system; v_s is the sound velocity derived from the derivative of the dispersion curve at $k = 0$; c is the central charge; η is the critical exponent defined by the spin-correlation function $\langle \tilde{s}_0^x \tilde{s}_r^x \rangle \sim r^{-\eta}$, where $\tilde{s}_i$ is some relevant spin operator. These equations are valid at gapless points. The values of c and η calculated for the systems $(3/2, 1)$ and $(2, 1)$ at $m = m_s$ and $m = m_s + 1$ indicate the following properties: as α decreases from 1 with fixed δ, the first and second plateaux vanish at the different Kosterlitz–Thouless critical points α_{c1} and α_{c2}, respectively, where η is 1/4 in both cases; the gapless spin-fluid phase characterized by $c = 1$ lies in the region $\alpha < \alpha_{c1}$ (α_{c2}) at $m = m_s$ ($m = m_s + 1$). The universal features of the phase boundaries of the two plateaux are the same as those of the unique plateau of the system $(1, 1/2)$ (Yamamoto and Sakai 1999, Sakai and Yamamoto 1999). Thus we determine that the gapless-plateau phase boundary has $\eta = 1/4$ for both plateaux. The thus-obtained phase boundaries for the first and second plateaux are shown together as solid lines in figures 4(a) and 4(b) for the systems $(3/2, 1)$ and $(2, 1)$, respectively. The phase diagrams obviously indicate the coexistence of the first (classical) and second (quantum) plateaux even at the most symmetric point ($\alpha = 1$ and $\delta = 0$). They also exhibit an interesting feature: the quantum plateau phase is larger than the classical one ($\alpha_{c1} \leqslant \alpha_{c2}$ independently of δ). This implies that the quantum plateau is more stable than the classical one against planar anisotropy.

So slight a size dependence of the scaled quantity $N\Delta_N(m)$ for the second plateau as that shown in figure 3(b) might make us doubt its existence for $\alpha = 1$ and $\delta = 0$. Thus we perform another type of analysis, called level spectroscopy (Okamoto and Nomura 1992, Nomura 1995), to convince ourselves of the existence of the second plateau. This type of analysis is one of the most precise methods for estimating the Kosterlitz–Thouless phase boundary. Since the method detects the boundary as a level crossing point for the two relevant excitation gaps with the same scaling dimension, the result does not suffer from the dominant logarithmic

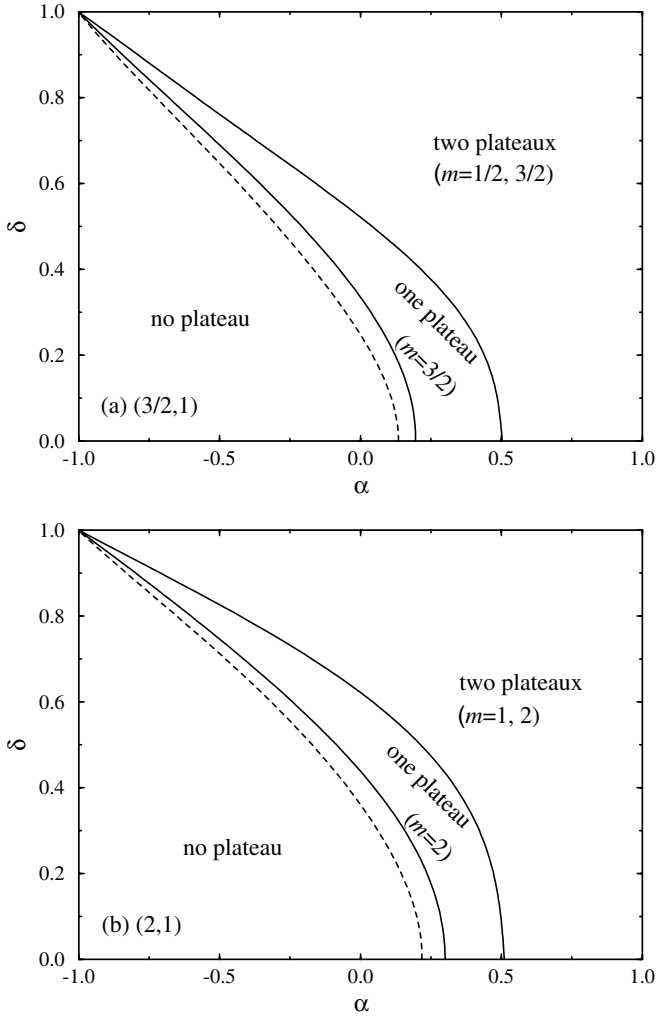

Figure 4. The ground-state phase diagrams in the α–δ plane for (a) (3/2, 1) and (b) (2, 1). Solid lines are the phase boundaries determined for $\eta = 1/4$. Dashed lines are the boundaries of the second plateaux determined by level spectroscopy. The small difference between the two sets of results for the second plateaux is due to the logarithmic size correction which should appear in the former method.

size correction, which is quite serious for the Kosterlitz–Thouless transition. For the second plateau at $m = S - s + 1$, the two relevant gaps are given by

$$\Delta_0 \equiv E_2(L, M_2) - E(L, M_2) \tag{7}$$

$$\Delta_4 \equiv [E(L, M_2 + 4) + E(L, M_2 - 4) - 2E(L, M_2)]/2 \tag{8}$$

where $E_2(L, M)$ is the second eigenvalue in the same subspace as $E(L, M)$ and M_2 is defined as $M_2 \equiv (S - s + 1)N$. The two excitations have the common scaling dimension 2. The values of Δ_0 and Δ_4 calculated for the system (3/2, 1) for $\delta = 0$ are plotted versus α in figure 5. This suggests that the phase boundary is easily determined as a crossing point, almost independently of the system size. The thus-obtained boundaries for the second plateaux are shown as dashed curves in figures 4(a) and 4(b). The results show a little deviation from the boundaries for

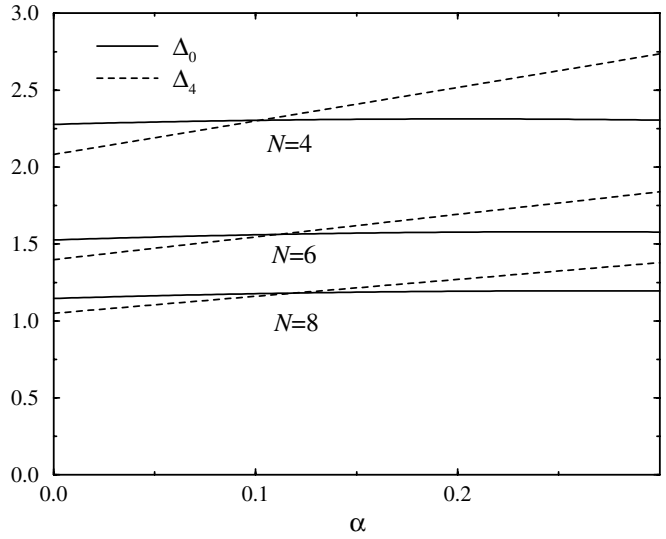

Figure 5. Δ_0 and Δ_4 for the system $(3/2, 1)$ with $\delta = 0$ versus α. This indicates that the crossing point of the two gaps is almost independent of the system size.

$\eta = 1/4$, because the latter includes the logarithmic size correction. Nonetheless they lead to the same conclusion: the coexistence of the classical and quantum plateaux for $\alpha = 1$ and $\delta = 0$.

The Néel–dimer crossover point in the first plateau indicated by the variational method in the previous section is not detected as any phase boundary by these numerical analyses. This suggests that the Néel and dimer pictures cannot be distinguished clearly for the first plateau. In fact it is trivially revealed that in the δ–α phase diagram at $m = m_s$ the isotropic dimer point ($\alpha = 1$ and $\delta = 1$) is connected to the Ising limit ($\alpha \to \infty$ and $\delta = 0$) via the Ising dimer limit ($\alpha \to \infty$ and $\delta = 1$) through no phase transition or crossover. This implies that the first plateau always has an aspect of the Ising gap even for large δ.

6. The magnetization curve

Finally we present the ground-state magnetization curve in several cases for the systems $(3/2, 1)$ and $(2, 1)$. The curve is given by extrapolating $H_{\pm}(N, M)$ to the thermodynamic limit using size scaling (Sakai and Takahashi 1998) based on conformal field theory at gapless points and the Shanks transformation for plateaux. We show only the results of a suitable polynomial fitting to the thus-obtained points, in figures 6 ($\delta = 0$) and 7 ($\delta = 0.4$), where the labels (a) and (b) indicate the systems $(3/2, 1)$ and $(2, 1)$, respectively. They show the coexistence of the classical and quantum plateaux at the Heisenberg point. These results also explain the above-mentioned feature: the quantum plateau is smaller at the Heisenberg point, but more stable against the XY-like anisotropy, than the classical one. Therefore, if these systems lose a plateau due to the anisotropy, only the quantum one will survive. In order to clarify the difference in the mechanism of gap formation between the first and second plateaux, we also present the magnetization curves of the classical Heisenberg spin systems described by the same Hamiltonian (2) with the same magnitudes $(S, s) = (3/2, 1)$ and $(2, 1)$ in figures 8(a) and 8(b), respectively. (The results are independent of δ.) The classical systems clearly have the first plateau in the isotropic case, while there is no plateau corresponding to the

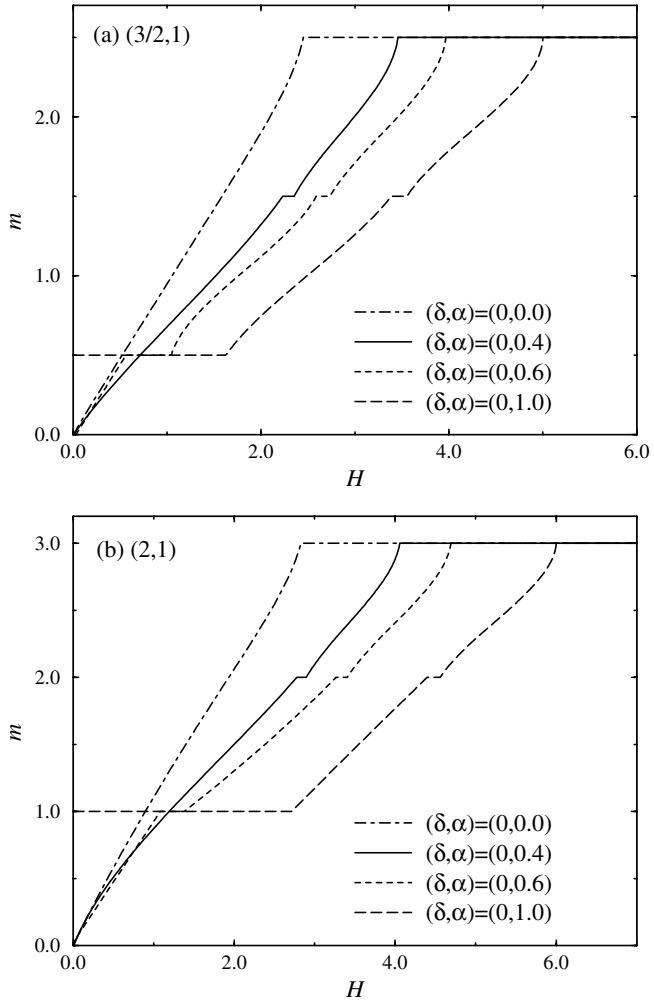

Figure 6. The ground-state magnetization curves of the quantum system with $\delta = 0$ at various values of α for (a) $(3/2, 1)$ and (b) $(2, 1)$.

second one. This also supports the assertion of a quantum nature of the second plateau. These plateaux of the classical systems vanish even for slight anisotropy: $\alpha_c = 0.980$ and 0.943 for $(S, s) = (3/2, 1)$ and $(2, 1)$, respectively. In comparison with these critical values, the phase boundaries in the quantum systems in figures 4(a) and 4(b) imply that quantum fluctuation stabilizes even the first plateau. Thus, in general, the quantum effect is expected to toughen every field-induced gap against planar anisotropy. Nevertheless, the first and second plateaux should be distinguished, because the former appears even in the classical limit, while the latter does not exist until the spin is quantized.

7. Concluding remarks

The above investigations indicate the coexistence of classical and quantum plateaux in the ground-state magnetization curve for the mixed-spin chains $(3/2, 1)$ and $(2, 1)$. This

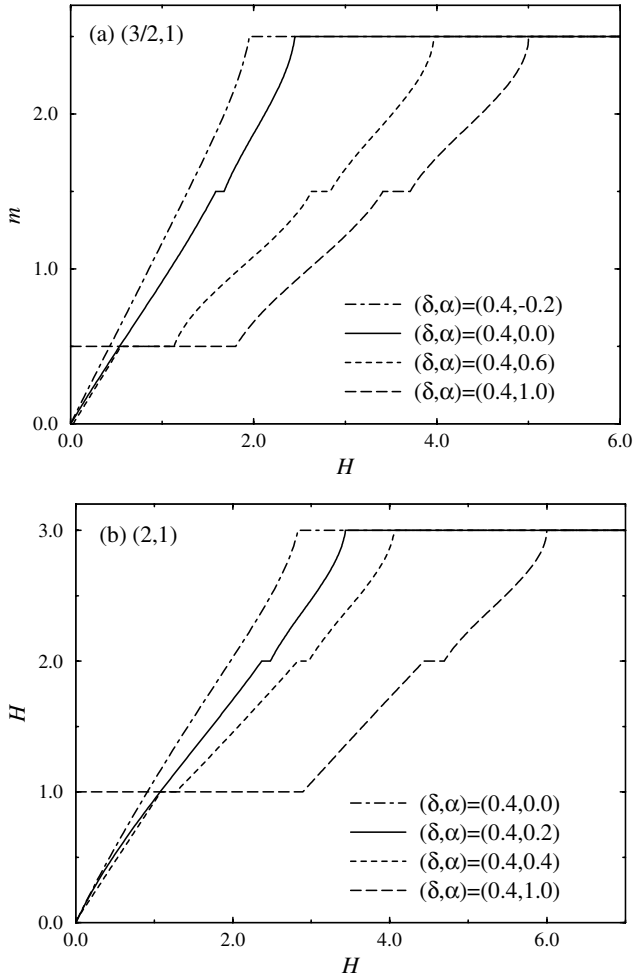

Figure 7. The ground-state magnetization curves of the quantum system with $\delta = 0.4$ at various values of α for (a) (3/2, 1) and (b) (2, 1).

conclusion is easily generalized for (S, s) $(S > s > 1/2)$; the magnetization curve has $2s$ plateaux and only the initial one is based on a classical mechanism, while the others originate from quantum correlations.

In most previous works on the magnetization plateau, the gap formation was based on bond polymerization (Totsuka 1998, Tonegawa *et al* 1996, Cabra *et al* 1997, Cabra and Grynberg 1999). In contrast, the present proposal for the plateau for ferrimagnetic chains is a pioneering attempt to explore a novel mechanism for producing the field-induced gap associated with *spin polymerization*. Bimetallic chains such as MM′(pbaOH)$(H_2O)_3 \cdot n H_2O$ (Kahn 1987, Kahn *et al* 1995) are good candidates for realizing spin polymerization. Unfortunately, most of them have M′ = Cu—that is, $s = 1/2$. In fact, a few compounds with other metals have also been synthesized—for example, MM′(EDTA)$\cdot 6H_2O$ (MM′ = CoNi, MnCo and MnNi). However, the case of MM′ = CoNi yields $(S, s) = (1(\mathrm{Ni}), 1/2(\mathrm{Co}))$ (Drillon *et al* 1985) and MnCo has a large Ising-like anisotropy (Drillon *et al* 1986). Thus they do not provide a suitable framework for searching for a quantum plateau. Among the series of bimetallic

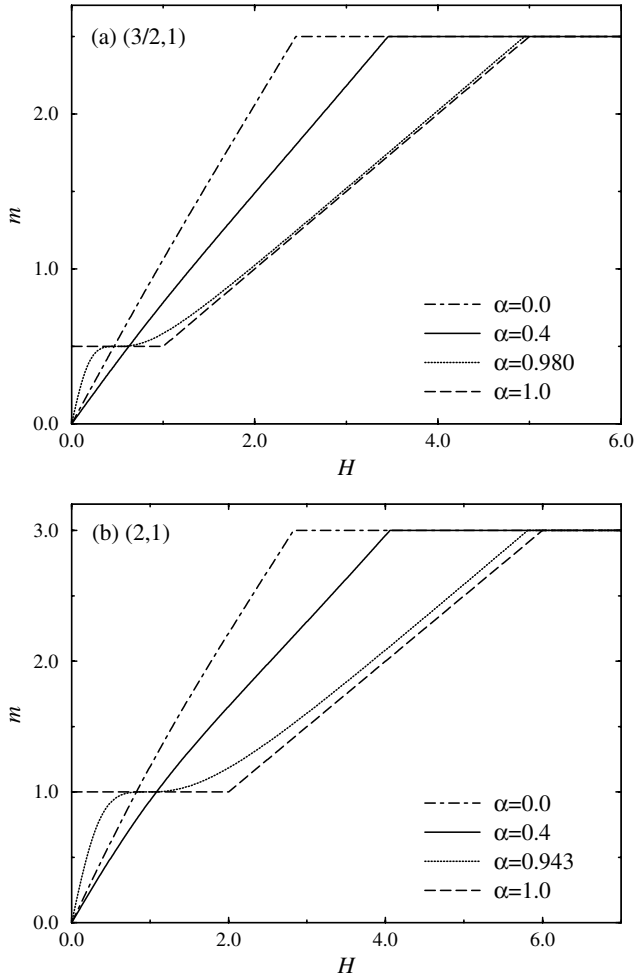

Figure 8. The ground-state magnetization curves of the classical system at various values of α for (a) $(3/2, 1)$ and (b) $(2, 1)$.

chains, the most suitable compound might be $MnNi(EDTA)\cdot 6H_2O$, which is well described by the 1D spin-alternating Heisenberg model for $(5/2, 1)$ (Drillon *et al* 1986). Magnetization measurements on this compound would be interesting for investigating a possible quantum plateau at $m = 5/2$, as well as the classical one at $m = 3/2$.

One of the most important findings in the present work is the coexistence of the quantum and classical plateaux even at the most symmetric point ($\alpha = 1$ and $\delta = 0$). In order to examine this feature, compounds consisting of metals and stable organic radicals (Caneschi *et al* 1989a, b, Markosyan *et al* 1998) might provide a more suitable framework—because the organic radicals lead to entirely isotropic spin systems—than the bimetallic chains with their inevitable Ising-like anisotropy. The metal–radical complex also has a lot of variations. The recently synthesized one $\{Mn(hfac)_2\}_3(3R)_2$ (Markosyan *et al* 1998) has been investigated with a view to realizing the $(5/2, 3/2)$ spin chain. We hope that the present calculations will stimulate not only further theoretical investigations, but also experimental explorations into the magnetization plateaux in ferrimagnets considered as spin-polymerized materials.

Acknowledgments

The authors thank Dr K Okamoto for useful discussion. This work was supported by the Japanese Ministry of Education, Science and Culture through Grant-in-Aid No 11740206 and by the Sanyo Broadcasting Foundation for Science and Culture. The computation was done in part using the facilities of the Supercomputer Centre, Institute for Solid State Physics, University of Tokyo.

References

Affleck I 1986 *Phys. Rev. Lett.* **56** 746
Blöte H W, Cardy J L and Nightingale M P 1986 *Phys. Rev. Lett.* **56** 742
Cabra D C and Grynberg M D 1999 *Phys. Rev. Lett.* **82** 1768
Cabra D C, Honecker A and Pujol P 1997 *Phys. Rev. Lett.* **79** 5126
Caneschi A, Gatteschi, Renard J-P, D, Ray P and Sessoli R 1989a *Inorg. Chem.* **28** 1976
Caneschi A, Gatteschi, Renard J-P, D, Ray P and Sessoli R 1989b *Inorg. Chem.* **28** 2940
Cardy J L 1984 *J. Phys. A: Math. Gen.* **17** L385
Drillon M, Coronado E, Beltran D, Curely J, Georges R, Nugteren P R, De Jongh L J and Genicon J L 1986 *J. Magn. Magn. Mater.* **54–57** 1507
Drillon M, Coronado E, Beltran D and Georges R 1985 *J. Appl. Phys.* **57** 3353
Kahn O 1987 *Struct. Bonding* **68** 89
Kahn O, Pei Y and Journaux Y 1995 *Inorganic Materials* ed D W Bruce and D O'Hare (New York: Wiley) p 95
Kuramoto T 1998 *J. Phys. Soc. Japan* **67** 1762
Markosyan A S, Hayamizu T, Iwamura H and Inoue K 1998 *J. Phys.: Condens. Matter* **10** 2323
Narumi Y, Hagiwara M, Sato R, Kindo K, Nakano H and Takahashi M 1998 *Physica* **246+247** 509
Nomura K 1995 *J. Phys. A: Math. Gen.* **28** 5451
Okamoto K and Nomura K 1992 *Phys. Lett.* A **169** 433
Oshikawa M, Yamanaka M and Affleck I 1997 *Phys. Rev. Lett.* **78** 1984
Sakai T and Takahashi M 1998 *Phys. Rev.* B **57** 3201
Sakai T and Yamamoto S 1999 *Phys. Rev.* B **60** 4053
Shiramura W, Takatsu K, Kurniawan B, Tanaka H, Uekusa H, Ohashi Y, Takizawa K, Mitamura and Goto T 1998 *J. Phys. Soc. Japan* **67** 1548
Tonegawa T, Nakao T and Kaburagi M 1996 *J. Phys. Soc. Japan* **65** 3317
Totsuka K 1998 *Phys. Rev.* B **57** 3454
Yamamoto S 2000 *Phys. Rev.* B **61** 842 and references therein
Yamamoto S and Sakai T 1999 *J. Phys.: Condens. Matter* **11** 5175